Excitonic-insulator instability and Peierls distortion in one-dimensional semimetals

Matteo Barborini [1,*] Matteo Calandra,[2,3] Francesco Mauri [4,5] Ludger Wirtz [1] and Pierluigi Cudazzo [1,†]

[1]*Department of Physics and Materials Science, University of Luxembourg, 162a avenue de la Faïencerie, L-1511 Luxembourg, Luxembourg*

[2]*Sorbonne Universités, CNRS, Institut des Nanosciences de Paris, UMR7588, 75252 Paris, France*

[3]*Dipartimento di Fisica, Università di Trento, Via Sommarive 14, 38123 Povo, Italy*

[4]*Dipartimento di Fisica, Università di Roma La Sapienza, Piazzale Aldo Moro 5, I-00185 Roma, Italy*

[5]*Graphene Labs, Fondazione Istituto Italiano di Tecnologia, Via Morego, I-16163 Genova, Italy*

(Received 15 June 2021; revised 21 September 2021; accepted 5 January 2022; published 10 February 2022)

The charge density wave instability in one-dimensional semimetals is usually explained through a Peierls-like mechanism, where the coupling of electrons and phonons induces a periodic lattice distortion along certain modes of vibration, leading to a gap opening in the electronic band structure and to a lowering of the symmetry of the lattice. In this work, we study two prototypical Peierls systems: the one-dimensional carbon chain and the monatomic hydrogen chain with accurate *ab initio* calculations based on quantum Monte Carlo and hybrid density functional theory. We demonstrate that in one-dimensional semimetals at $T = 0$, a purely electronic instability can exist independently of a lattice distortion. It is induced by spontaneous formation of low energy electron-hole pairs resulting in the electronic band gap opening, i.e., the destabilization of the semimetallic phase is due to an excitonic mechanism.

DOI: 10.1103/PhysRevB.105.075122

I. INTRODUCTION

The static charge density wave (CDW) regime is a broken symmetry state induced by electron-phonon or electron-electron interactions. It can occur in certain semimetals when cooled down below a given critical temperature. In this state, the charge density is not uniform, but displays a spatial oscillation that is, generally, accompanied by a periodic lattice distortion (PLD) so that it is often referred to as CDW/PLD [1]. Even if CDW/PLD dates back to the early days of quantum mechanics [2,3], it is still nowadays a fascinating and not completely understood research topic. Indeed, even though in several classes of materials displaying CDW/PLD order much has been understood about the structural and electronic properties and about the nature of the CDW/PLD phases, we are still far from understanding how and why CDW/PLDs are formed.

Common phenomenological models used to describe the CDW/PLD phase transition are the Peierls mechanism and the Jahn-Teller effect. In both cases the driving force responsible for the CDW/PLD order is the electron-phonon interaction, in contrast with a purely electronic mechanism [4] also called excitonic insulator (EI), that could develop in both semimetals and semiconductors [5–7]. In this case, due to the attractive electron-hole (e-h) interaction induced by exchange-correlation (xc) effects, bound e-h pairs (excitons) can be formed spontaneously at zero energy cost if the exciton binding energy is large enough. The instability towards the spontaneous formation of e-h pairs results in the softening of an exciton or plasmon mode that is accompanied by the formation of a CDW as well as by a change of the electronic band structure. In addition, the electric field caused by the CDW in general leads to the displacement of the positive ions from their ideal equilibrium positions (i.e., the positions before the distortion) giving rise to a PLD.

After its theoretical prediction, the EI phase has been intensively searched in different kinds of materials such as semimetals [8–10], photoexcited semiconductors [11], as well as two-dimensional systems [12,13] and single wall carbon nanotubes [14,15]. Nevertheless, despite the great efforts, a conclusive experimental evidence for the existence of this phase remains elusive.

Among CDW/PLD systems, the simplest and most studied ones are probably the one-dimensional (1D) atomic chains. They are prototypical Peierls unstable systems where the instability arises from the cooperation between the perfect Fermi surface nesting and electron-phonon interaction and represent standard textbook examples to explain the CDW/PLD physics. However, the Peierls mechanism has been questioned in several works that, based on model Hamiltonians, speculated about the possibility that in 1D semimetals such as polyacene based systems the CDW/PLD has a purely electronic nature [16–18].

In this paper we address again the basic academic question concerning the physical origin of the CDW in 1D systems. Combining fully *ab initio* calculations based on quantum Monte Carlo (QMC) and density functional theory (DFT) we investigate the CDW/PLD in two prototypical 1D systems: the carbon chain, namely, cumulene (CU), which is predicted to dimerize through a Peierls mechanism in the most stable polyyne conformation (PO), and the monatomic hydrogen chain, that with a single half-filled band constitutes the simplest 1D material and thus a suitable model system to investigate the basic CDW physics. We demonstrate that

*Corresponding author: matteo.barborini@uni.lu

†Corresponding author: pierluigi.cudazzo@uni.lu

in these materials, in contrast to the previous interpretations, there is a CDW of purely electronic origin, followed by a PLD due to the electron-phonon interaction.

II. COMPUTATIONAL METHODS

A. Quantum Monte Carlo

The *ab initio* QMC calculations [19–21] are performed with the TURBORVB package [22]. In particular, the method used to optimize the wave function and the structural parameters and used to compute the forces and total energies is that of variational Monte Carlo (VMC). In the rest of the paper we will use in general the term QMC. The electronic structure of our system is described through variationally optimized wave functions built as the product of the antisymmetrized geminal power (AGP) [23,24] ansatz and a Jastrow factor [25]. The AGP wave function is derived from the BCS theory of superconductivity [26–28] and explicitly describes the correlation between electron pairs [23,24,29,30]. For closed shell systems the AGP is the determinant of a $N_e^{\uparrow} \times N_e^{\downarrow}$ square matrix $\mathbf{G}$: $\Phi_{\mathrm{AGP}}(\bar{\mathbf{x}}) = \det[\mathbf{G}]$ whose elements $\mathbf{G}_{ij} = \phi_G(\mathbf{r}_i^{\uparrow}, \mathbf{r}_j^{\downarrow})$ are geminal pairing functions that couple electrons of opposite spin in an antisymmetric state. The spatial part of the geminal functions is a linear combination of products of two atomic orbitals weighted by a set of coefficients,

$$\phi_G(\mathbf{r}_i^{\uparrow}, \mathbf{r}_j^{\downarrow}) = \sum_{q,p=1}^{Q} \lambda_{qp} \phi_q(\mathbf{r}_i^{\uparrow}) \phi_p(\mathbf{r}_j^{\downarrow}),$$

multiplied by a spin-antisymmetric singlet state. For a spin restricted calculation the coefficients λ_{qp} must be symmetric ($\lambda_{qp} = \lambda_{pq}$) in order to guarantee that the spatial part is symmetric with respect to the exchange of the two electrons' coordinates. It has been shown that the AGP can be rewritten as a multideterminantal expansion of a full set of constrained excitations and in particular it is able to describe properly diradical configurations of an even number of degenerate frontier states [31–33]. The Jastrow factor [34] used contains the homogeneous two body and one body terms necessary for describing correctly the electron-electron and electron-nucleus cusp conditions (used for the hydrogen chain), and three/four body terms that describe the electronic correlation between the electron pairs with respect to the positions of one or two nuclei. This last factor is important to recover a high level of dynamical correlation between electron pairs [25].

We have used localized basis sets for both the AGP wave function and for the dynamical part of the Jastrow factor. The AGP basis set for the carbon atoms corresponds to a combination of contracted Gaussian type orbitals (GTOs), $(5s5p2d)/[2s2p1d]$, while for the hydrogen atoms it corresponds to a combination of Gaussian and Slater type orbitals (STOs), $(2s1s^*1p^*)/[1s1s^*1p^*]$ (the asterisk indicates the uncontracted STO orbitals). The basis set used to build the dynamical part of the Jastrow factor is composed of pure uncontracted GTOs: $(2s2p1d)$ for the carbon atoms and $(2s1p)$ for the hydrogen ones. The $1s$ core electrons of the carbon atoms are substituted through energy-consistent pseudopotentials with relativistic corrections [35].

In order to describe the infinite chains with QMC, we have used periodic boundary conditions [29] extrapolating the results to the infinite supercell limit. For each supercell, with number of atoms $N_{\mathrm{C}} \in [8:40]$ and $N_{\mathrm{H}} \in [8:48]$, we have optimized the wave functions with the linear method [36,37] with Hessian acceleration as described in Ref. [38], and the structural geometries with the method described in Refs. [39,40]. The infinite length extrapolations are done using the function $f(x) = a + bx^c$ (with $x = 1/N$) that for long enough cells reduces to a second order polynomial $c = 2$.

B. Density functional theory

The DFT calculations presented in this work have been done with the CRYSTAL17 program [41] using the pob-TZVP basis set [42] built of localized Gaussian type orbitals and optimized to guarantee reasonably converged results on periodic systems. All the calculations have been done with 300 k points in the irreducible Brillouin zone using the long-range corrected CAM-B3LYP hybrid xc functional [43]:

$$\begin{aligned} E_{xc} = E_{xc}^{L} &+ \alpha_0 \left[E_{x,SR}^{NL}(\omega) - E_{x,SR}^{L}(\omega) \right] \\ &+ \alpha \left[E_{x,LR}^{NL}(\omega) - E_{x,LR}^{L}(\omega) \right], \end{aligned} \tag{1}$$

where E_{xc}^{L} is the local xc functional evaluated in generalized gradient approximation (GGA), E_x^L its exchange counterpart, and E_x^{NL} the nonlocal exchange correction evaluated in the Hartree Fock (HF) approximation. Both, local and nonlocal exchange functionals are separated in a short-range and long-range contribution whose length scale is set by ω according to the following representation of the Coulomb potential:

$$\frac{1}{|\mathbf{r} - \mathbf{r}'|} = \underbrace{\frac{1 - \mathrm{erf}(\omega |\mathbf{r} - \mathbf{r}'|)}{|\mathbf{r} - \mathbf{r}'|}}_{SR} + \underbrace{\frac{\mathrm{erf}(\omega |\mathbf{r} - \mathbf{r}'|)}{|\mathbf{r} - \mathbf{r}'|}}_{LR}, \tag{2}$$

where erf denotes the error function.

III. RESULTS AND DISCUSSION

The Peierls mechanism for CU is schematically represented in Fig. 1. Here the sp hybridization results in the formation of a σ covalent bond and a metalliclike bond with mixed π_x-π_y character which gives rise to the formation of a twofold degenerate metallic band [Fig. 1(a)].

After dimerization [see Fig. 1(b)], a configuration with an alternating single covalent σ bond and triple (σ plus mixed π_x-π_y) covalent bonds becomes energetically favored with respect to the previous homogeneous electronic configuration and a gap opens at the boundary of the first Brillouin zone (BZ) at $\mathbf{k} = \frac{\pi}{2a}$ (a being the lattice constant). The resulting CDW/PLD phase (or PO phase) with wave vector $\mathbf{q} = \frac{\pi}{a}$ is described by a new unit cell with two carbon atoms and a finite bond length alternation (BLA): the difference between the lengths of the singlet and triplet bonds.

In the alternative EI picture, xc effects induce the spontaneous formation of bound e-h pairs with relative wave vector $\mathbf{q} = \frac{\pi}{a}$. They involve transitions around the Fermi surface from $\mathbf{k} = -\frac{\pi}{2a}$ to $\mathbf{k} = \frac{\pi}{2a}$. Equivalently, if described using a supercell made of two carbon atoms (folding $\mathbf{q}$ onto the Γ point), there will be vertical transitions at the boundary of the BZ [see Fig. 1(c)]. This gives rise to a CDW with wave vector $\mathbf{q} = \frac{\pi}{a}$ opening a gap at the BZ boundary [see Fig. 1(d)]. In

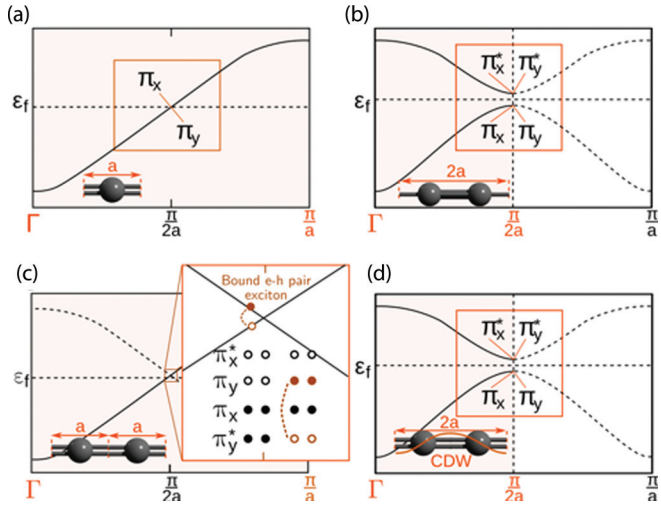

FIG. 1. (a) Band structure of cumulene, containing a single carbon atom per unit cell. (b) Band structure of polyyne, containing two atoms per unit cell. (c) Excitonic effect in cumulene. (d) CDW band structure: the gap opens because of exciton formation.

the following we will call this hypothetical phase EI CDW. Obviously, this purely electronic CDW induces a PLD that will drive the system into a more stable structure.

In order to verify this hypothesis we employ *ab initio* QMC calculations using the scheme discussed in Sec. II. The structural parameters of CU and PO have been obtained through a supercell approach and extrapolating to the thermodynamic limit ($N_C \to \infty$). Moreover for each supercell we have optimized the wave function and the atomic positions. Our results are summarized in Table I. The value of the BLA is around 0.1363(12) Å and compatible with those obtained both experimentally and through DFT calculations [44–48] as well as more recent diffusion Monte Carlo (DMC) calculations [49]. Albeit, our extracted lattice constant of PO [2.5649(4) Å] is slightly smaller than the value of 2.582 Å reported in Ref. [49] probably due to the different pseudopotentials used in our work. In fact, it has been shown in other works [40] that the energy-consistent pseudopotentials in Ref. [35] tend to shorten the carbon lengths with respect to the norm-conserving ones.

TABLE I. Structural properties of the carbon chain per supercell. N_C is the number of carbon atoms, a_{PO} and BLA_{PO} are, respectively, the lattice constant and the bond length alternation of polyyne, and a_{CU} is the lattice constant of cumulene.

N_C	a_{PO} (Å)	BLA_{PO} (Å)	a_{CU} (Å)
8	2.5898(5)	0.1900(7)	2.5664(5)
12	2.5731(5)	0.1586(7)	2.5549(5)
16	2.5681(5)	0.1455(7)	2.5501(5)
24	2.5653(5)	0.1399(7)	2.5472(5)
32	2.5660(5)	0.1386(7)	2.5470(5)
40	2.5652(5)	0.1383(7)	
∞	2.5649(4)	0.1363(12)	2.5454(7)

TABLE II. Energies per pseudocarbon atom in Hartree (Ha) as a function of the supercell. N_C is the number of carbon atoms and E_{PO}, E_{CU} and $E_{EI\,CDW}$ are, respectively, the energies of polyyne, cumulene, and the EI CDW state.

N_C	E_{PO}/N_C (Ha)	$E_{EI\,CDW}/N_C$ (Ha)	E_{CU}/N_C [Ha]
8	−5.64448(6)	−5.63343(7)	−5.62704(5)
12	−5.64698(4)	−5.64024(5)	−5.63605(3)
16	−5.64734(4)	−5.64214(4)	−5.63921(3)
24	−5.64757(3)	−5.64321(4)	−5.64129(3)
32	−5.64741(3)	−5.64336(2)	−5.64192(2)
40	−5.64750(2)	−5.64358(3)	−5.64211(2)
∞	−5.64750(4)	−5.64363(5)	−5.64266(8)

For each optimized structure we report the variational energies per pseudocarbon atom in Table II for the PO and CU phases extrapolated to the thermodynamic limit ($N_C \to \infty$).

The ground state energies, derived by extrapolation to the thermodynamic limit, clearly show that PO is the most stable phase [see Fig. 2(a)]. Interestingly, by removing all the symmetries on the electronic wave function, but taking the

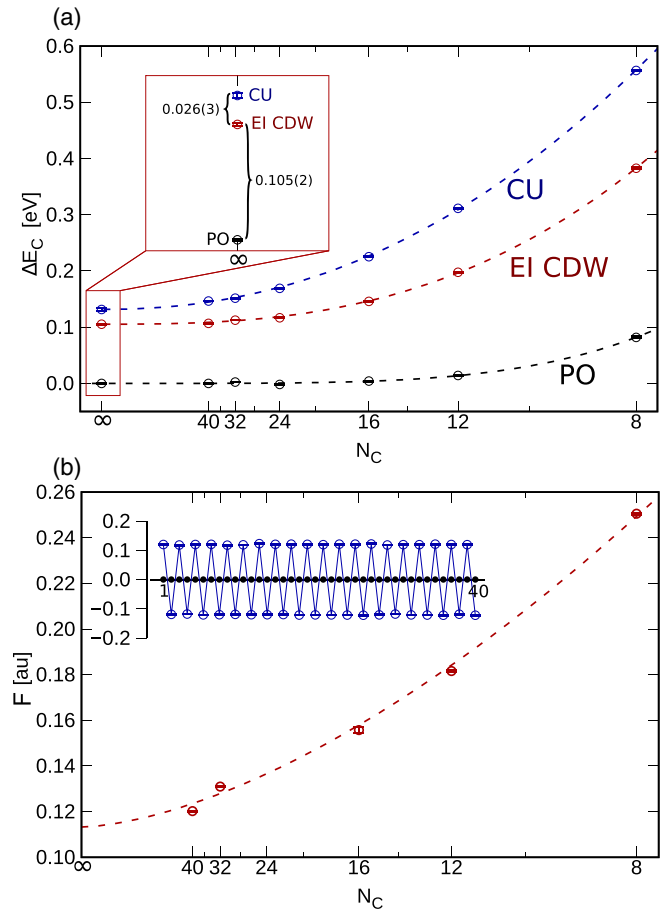

FIG. 2. QMC calculations for the carbon chain. (a) Extrapolations of atomic energies as a function of the supercell's length for CU, EI CDW, and PO states. In the inset the energy differences are reported in eV with respect to the two atom PO cell. (b) Residual forces in the EI CDW state per atom. In the inset the residual forces for a 40 carbon atom supercell.

carbon atoms fixed at the ideal positions of the CU structure, the system spontaneously evolves into a new electronic configuration with an energy gain of about 0.026(3) eV per carbon atom with respect to the ideal CU configuration [see red curve in Fig. 2(a)].

This state can be characterized by evaluating the absolute values of the forces acting on the single carbon atoms along the molecular axis [Fig. 2(b)]. These values extrapolate to a positive quantity in the thermodynamic limit. In the inset of Fig. 2(b), for a 40 carbon atom supercell we recognize how the atomic forces have the same intensity but opposite sign on adjacent atoms: a profile compatible with the PLD associated to the PO structure. This behavior is a signature of an EI CDW state that pushes the symmetric structure of CU towards the PO minimum. The same behavior is found for the hydrogen chain, suggesting that the excitonic instability is an intrinsic property of quasi-1D semimetals (see Appendix A).

In the following, to gain further insight into the physical mechanism governing the EI CDW instability observed in QMC calculations, we address this problem in the DFT framework using the hybrid long-range corrected CAM-B3LYP xc functional [43], that has been shown to compare well with QMC in conjugated carbon chains [32,50].

In the calculations we keep the amount of short-range nonlocal HF exchange α_0 fixed at the standard value of 0.16 and optimize $\alpha \in [0, 1]$ (i.e., the amount of the long-range nonlocal HF exchange) in order to match the QMC ground state. Moreover we keep the length scale ω of the nonlocal correction fixed at the standard value of 0.33 for both short- and long-range contributions. The traditional GGA approximation is recovered for $\alpha = \alpha_0 = 0.0$ while the best agreement with the QMC results (i.e., the energy difference between PO and CU phases and the values of the BLA and lattice constant) are obtained for $\alpha \approx 0.7$ (see Appendix A). In order to investigate the EI CDW phase observed in the QMC calculations, we simulated the CU carbon chain using a supercell consisting of two equivalent atoms in the presence of an external perturbative field $\Delta_{\text{ext}}(\mathbf{r})$ characterized by the same symmetry as that of the expected CDW order. The perturbation $\Delta_{\text{ext}}(\mathbf{r})$ is introduced to break the symmetry and is afterwards put to zero, simulating spontaneous symmetry breaking. For $\alpha = 0$ (i.e., in standard GGA approximation for the long-range part of the exchange interaction) the CDW is only observed in the presence of a PLD [$\Delta_{\text{ext}}(\mathbf{r}) > 0$] while for $\alpha > 0$, a new phase, with the ions fixed at the same positions of the ideal CU structure, is stabilized with respect to the semimetallic CU phase, in qualitative agreement with QMC. This phase, characterized by a charge modulation with wave vector $\mathbf{q} = \frac{\pi}{a}$ and an energy gap at the boundary of the BZ that increases as a function of α [blue circles in Fig. 3(a)], is a clear evidence of the EI CDW. Interestingly, when the spin degrees of freedom are allowed to relax, the system spontaneously evolves into a spin density wave (SDW) phase with the same periodicity of the CDW order. The antiferromagnetic band gap takes a finite value also for $\alpha \to 0$ and is always larger then the EI CDW energy gap for all values of α [see Fig. 3(a)] suggesting that the SDW is actually more stable than the EI CDW phase. However, when ions are allowed to relax into the new equilibrium configuration, the PO structure is obtained (i.e., CDW/PLD phase) and the CDW ordering is stabilized

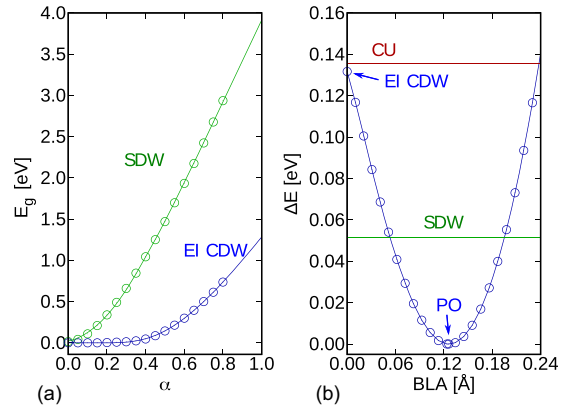

FIG. 3. (a) Band gap E_g as a function of α for the EI CDW (blue circles) and SDW (green circles) phases of the carbon chain. The continuous line is the fit of the *ab initio* data through Eq. (7). (b) Ground state energy of the CDW/PLD phase of the carbon chain as a function of the BLA evaluated at $\alpha = 0.7$. The red and green lines refer to the energy of the CU and SDW phases, respectively. In the plot the zero is fixed at the energy of the PO phase.

with respect to the SDW [see Fig. 3(b)]. The same behavior is observed also for the hydrogen chain suggesting that in these materials the destabilization of the semimetallic phase is purely electronic and we do not need to invoke the electron-phonon coupling, in contrast to the pure Peierls mechanism. Nevertheless, the electron-phonon coupling is essential to stabilize the CDW with respect to SDW. Again, this same effect is also observed for the hydrogen chain (Appendix A).

In order to make a direct link between our *ab initio* results and the EI picture, it is helpful to separate the Kohn-Sham (KS) Hamiltonian corresponding to the broken symmetry phase into two parts: the unperturbed one ($h^0[\rho_0]$) describing the ideal monatomic chain with unperturbed charge density ρ_0 and a perturbative term $\Delta h[\rho_0, \Delta\rho]$ describing the self-consistent field associated to the induced charge density $\Delta\rho$ (see Appendix B for further details):

$$\hat{H} = \sum_{ij\mathbf{k}} \left(\epsilon^0_{i\mathbf{k}}\delta_{ij} + \Delta h_{i\mathbf{k},j\mathbf{k}}\right) c^\dagger_{i\mathbf{k}} c_{j\mathbf{k}} + \Delta h_{i\mathbf{k},j\mathbf{k}+\mathbf{q}} c^\dagger_{i\mathbf{k}} c_{j\mathbf{k}+\mathbf{q}}, \quad (3)$$

where $\mathbf{k}$ runs over the first BZ, corresponding to the unperturbed configuration, $i(j)$ are band indexes, $\mathbf{q}$ is the wave vector of the CDW, and the ϵ^0 are the eigenvalues of h^0. In the case of the hydrogen chain, when the coupling between the band crossing the Fermi level and higher energy empty bands is neglected, Eq. (3) can be diagonalized through a Bogoliubov–de Gennes transformation. For small Δh, the KS eigenvalues of $\hat{H}$ can be expressed in terms of ϵ^0 through the relation $\epsilon^\pm_{\mathbf{k}} = \xi_{\mathbf{k}} \pm E_{\mathbf{k}}$, where now $\mathbf{k}$ runs over the first BZ associated to the supercell folding $\mathbf{q}$ at the Γ point, $E_{\mathbf{k}} = \sqrt{\xi^2_{\mathbf{k}} + \Delta^2_{\mathbf{k}}}$ and $\xi_{\mathbf{k}} = \frac{1}{2}(\epsilon^0_{c\mathbf{k}} - \epsilon^0_{v\mathbf{k}})$, v (c) labeling occupied (empty) states of h^0. The quantity $\Delta_{\mathbf{k}}$ is directly related to the KS gap (E_g) of the CDW phase through the relation $E_g = 2\Delta$ (Δ being the value of $\Delta_{\mathbf{k}}$ at the boundary of the BZ) and satisfies the following BCS-like equation (see Appendix B):

$$\Delta_{\mathbf{k}} = -\frac{1}{2}\sum_{\mathbf{k}'} \mathcal{K}_{\mathbf{k},\mathbf{k}'} \frac{\Delta_{\mathbf{k}'}}{E_{\mathbf{k}'}}. \quad (4)$$

Here the kernel $\mathcal{K}$ is obtained from the functional derivative of the Hartree and xc potentials with respect to the electronic density and can be formally written as the sum of a nonlocal exchange kernel f_x^{NL} entering as a direct e-h interaction and a term entering as an exchange e-h interaction consisting of the Coulomb potential v, the local xc kernel f_{xc}^{L}, and its exchange part f_x^L [51] (here in order to simplify the discussion we drop the short-range nonlocal correction proportional to α_0):

$$\mathcal{K}_{\mathbf{k},\mathbf{k}'} = 2v_{\mathbf{k},\mathbf{k}'} + f^L_{xc\mathbf{k},\mathbf{k}'} - \alpha f^L_{x\mathbf{k},\mathbf{k}'}(\omega) + \alpha f^{NL}_{x\mathbf{k},\mathbf{k}'}(\omega). \quad (5)$$

Moreover, taking into account only the linear terms in $\Delta\rho$, we find that the energy gain associated to the CDW order is given by the expression $\Delta E = \sum_{\mathbf{k}}(E_{\mathbf{k}} - \xi_{\mathbf{k}})$. This means that the CDW phase is stable if Eq. (4) allows a nontrivial solution and thus the quantity $\Delta_{\mathbf{k}}$ can be interpreted as the order parameter of the CDW phase transition.

This simplified picture is valid for the carbon chain as well. Indeed, even if CU is a multiband system consisting of two degenerate bands crossing the Fermi level, the symmetry of the CDW allows only for intraband coupling. As a consequence the CDW is described through two equivalent BCS-like equations involving π_x and π_y states, respectively. This can be easily understood from the fact that the π_x-π_y degeneration persists in the CDW phase.

At this point, following Ref. [6], we make the change of variable $\varphi_{\mathbf{k}} = \frac{\Delta_{\mathbf{k}}}{E_{\mathbf{k}}}$ in Eq. (4) and, taking the limit $\Delta_{\mathbf{k}} \to 0$, we recover the Casida equation for the charge-charge response function $\chi(\mathbf{q},\omega)$ in the Tamm-Dancoff approximation [52]:

$$\left[\left(\epsilon^0_{c\mathbf{k}} - \epsilon^0_{v\mathbf{k}}\right) + o(\Delta^2)\right]\varphi_{\mathbf{k}} + \sum_{\mathbf{k}} \mathcal{K}_{\mathbf{k},\mathbf{k}'}\varphi_{\mathbf{k}'} = 0. \quad (6)$$

A comparison of Eq. (6) with Eq. (4) clearly shows that nontrivial solutions of Eq. (4) exist if χ presents poles at negative energies (i.e., softening of exciton modes). In the present case, since the KS as well as the quasiparticle gap of the unperturbed system is zero by symmetry, the condition for the stability of the CDW phase reduces to the existence of a bound state (i.e., a pole below the Fermi level).

For $\alpha \to 0$ the long-range xc part of $\mathcal{K}$ reduces to f_{xc}^L. Under these conditions, in line with previous studies on 1D systems [53], the CDW is always unstable. Indeed, it is well known that local approximations for the xc kernel [such as GGA or local density approximation (LDA)], being $\mathbf{q}$ independent, cannot describe bound excitons in infinite semiconductors (or semimetals) [54,55]. This is a consequence of the nonphysical behavior of their matrix elements between electronic wave functions that vanish in the optical limit ($\mathbf{q} \to 0$). In other words, the formation of a bound state is prevented by the presence of the dominant repulsive term v in Eq. (5). This does not happen for triplet excitations due to the lack of v. As a consequence, the SDW instability persists also for $\alpha \to 0$. On the other hand, in the opposite limit (i.e., $\alpha \to 1$, $\omega \to \infty$, and $f_{xc}^L = 0$) we recover the time-dependent HF approximation. In this case, bound excitons are allowed due to the singularity of the direct e-h interaction ($f^{NL}_{x\mathbf{k},\mathbf{k}'}$) for $\mathbf{k} = \mathbf{k}'$ that dominates on the v term. This is the physical origin of the Overhauser instability of the three-dimensional homogeneous electron gas [4] or the singlet state instability observed in 1D systems in the HF approximation [56].

However, in metallic systems the singularity in the direct e-h interaction is removed when long-range screening effects are taken into account and the CDW instability is expected to be suppressed. This is consistent with the common idea that excitonic effects are negligible in standard metals. Interestingly, in the present case the inclusion of correlation effects beyond the HF approximation does not remove the CDW instability. This is strictly related to the suppression of the long-range screening in low-dimensional systems that ensures a strong e-h interaction even when screening effects are properly taken into account.

To better understand the behavior of the KS gap as a function of α in Fig. 3(b), we now consider a simplified model where the kernel of Eq. (4) is assumed to be $\mathbf{k}$ independent. In particular, we take $\mathcal{K}_{\mathbf{k},\mathbf{k}'} = \bar{\mathcal{K}}$ inside an energy window ξ_0 around the Fermi level and $\mathcal{K}_{\mathbf{k},\mathbf{k}'} = 0$ elsewhere. The quantity $\bar{\mathcal{K}}$ is the average value of the kernel around the Fermi surface. Moreover we take a linear dispersion for the eigenvalues of h_0 so that $\xi_{\mathbf{k}} = v_F(|\mathbf{k}| - \frac{\pi}{a})$, v_F being the Fermi velocity. This is a good approximation as long as ξ_0 is small with respect to the band width. Under these conditions Eq. (4) has a simple BCS-like solution of the form (see Appendix B)

$$\Delta = \begin{cases} -\frac{\xi_0}{\sinh(\frac{\gamma}{\beta-\alpha})} & \text{for } \alpha > \beta, \xi_{\mathbf{k}} \leqslant \xi_0 \\ 0 & \text{for } \alpha \leqslant \beta, \xi_{\mathbf{k}} > \xi_0 \end{cases}, \quad (7)$$

where the parameters ξ_0, γ, and β can be estimated through interpolation of the *ab initio* results. For the CDW gap we find $\xi_0 = 2.14\,\text{eV}$, $\gamma = 1.84$, and $\beta = 0.05$. The last quantity sets the critical value of α for the CDW transition highlighting the fact that in these materials a pure electronic instability is present also for a weak direct e-h interaction. The physical origin of this behavior can be ascribed to the presence of a perfect nesting in the Fermi surface of 1D metals, that allows for the formation e-h pairs around the Fermi level with zero kinetic energy cost. This enables the formation of bound states even when the effect of the singularity in $f_x^{NL}(\omega)$ is strongly reduced (i.e., small values of α). Finally, for the SDW gap we find $\xi_0 = 3.92\,\text{eV}$, $\gamma = 1.84$, and $\beta = -0.28$. This is consistent with the fact that the SDW is stable for any positive α due to the lack of the repulsive interaction v in the kernel of the gap equation.

IV. CONCLUSIONS

In conclusion, performing a fully *ab initio* study of two prototypical 1D systems, namely, the CU phase of the linear carbon chain and the linear hydrogen chain, we have demonstrated that the CDW/PLD phase transition in 1D monatomic chains has a purely electronic origin. In particular, in analogy with the Peierls mechanism, the physical origin of the instability is the perfect nesting of the 1D Fermi surface. However, the driving force is the exchange Coulomb interaction instead of the electron-phonon interaction invoked in the Peierls mechanism. The latter comes in addition and stabilizes the CDW/PLD with respect to the SDW. Our findings suggest that the destabilization of the semimetallic phase of these materials has an excitonic origin. It should be pointed out, however, that although the driving force may be different, the outcome of the Peierls and EI instabilities is qualitatively the

TABLE III. Structural properties of the hydrogen chain per supercell. N_H is the number of hydrogen atoms, a_{ME} is the optimized lattice constant for the equally spaced hydrogen chain, and BLA_{DI} is the relaxed bond length alternation after dimerizaion.

N_H	a_{ME} (Å)	BLA_{DI} (Å)
8	2.0586(4)	0.6332(3)
12	2.0014(4)	0.5715(3)
16	1.9809(4)	0.5521(3)
24	1.9655(4)	0.5381(3)
32	1.9613(4)	0.5346(3)
48	1.9573(4)	0.5312(3)
∞	1.9541(5)	0.5293(4)

same: a novel ground state with lower symmetry exhibiting a CDW, a PLD, and a gap in the electronic band structure. Moreover, the two scenarios are mathematically described in a similar way.

ACKNOWLEDGMENTS

We acknowledge financial support from Agence Nationale de la Recherche (Grant No. ANR-19-CE24-0028) and the Fond National de Recherche, Luxembourg via project INTER/19/ANR/13376969/ACCEPT.

APPENDIX A: THE HYDROGEN CHAIN

The same information computed for the carbon chain has also been obtained for the hydrogen one as summarized in Table III. For this system we have first optimized the wave functions and the lattice constant of the semimetallic chain with equidistant hydrogens. Afterwards, we have optimized the BLA keeping the lattice constant fixed. The extrapolation of the geometrical parameters to the thermodynamic limit is reported in the last line of Table III. We must point out that the dimerized configuration is not in its equilibrium geometry, since this would correspond to infinitely distant hydrogen molecules distributed along the chain's axis. On the structural parameters we have computed the variational energies per atom for each supercell, which are reported in Table IV for the three phases: the metallic (ME) phase, the EI CDW phase, and the dimerized (DI) phase. The extrapolated results are listed in the last line of the table, and are obtained through

TABLE IV. Energies per hydrogen atom in Hartree (Ha) as a function of the supercell. N_H is the number of hydrogen atoms in the supercell and E_{DI}, E_{ME}, and $E_{EI\,CDW}$ are the energies per atom, respectively, of the dimerized, the metallic, and the EI CDW phases.

N_H	E_{DI}/N_H (Ha)	$E_{EI\,CDW}/N_H$ (Ha)	E_{ME}/N_H (Ha)
8	−0.579532(14)	−0.555744(11)	−0.551108(16)
12	−0.578497(9)	−0.560319(7)	−0.558347(13)
16	−0.578062(8)	−0.562296(7)	−0.560842(11)
24	−0.577459(7)	−0.563473(6)	−0.562658(9)
32	−0.577396(7)	−0.563974(5)	−0.563132(7)
48	−0.577227(6)	−0.564215(4)	−0.563583(6)
∞	−0.57723(7)	−0.56447(5)	−0.56397(4)

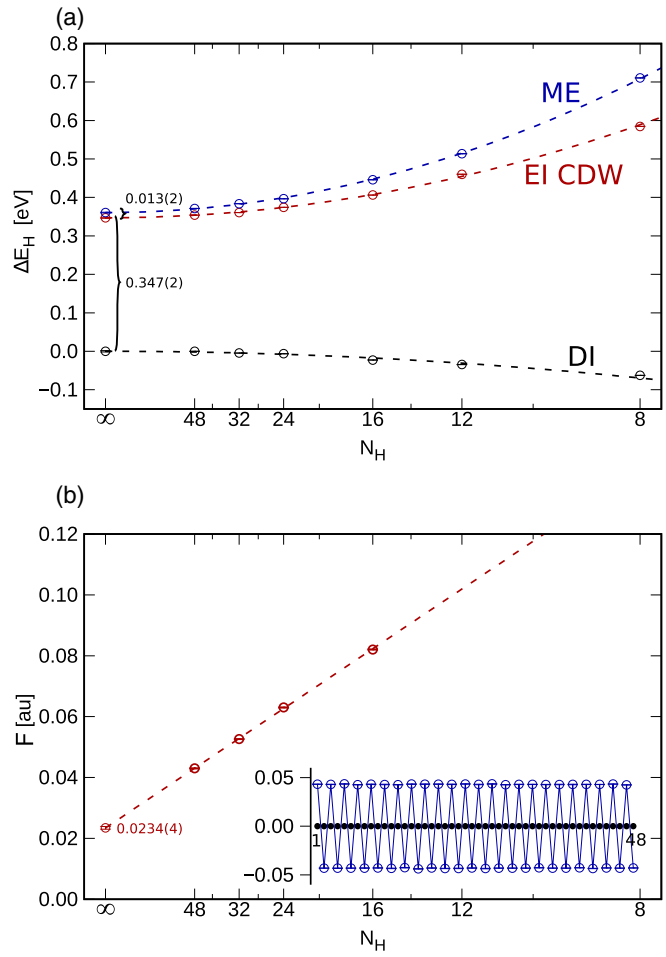

FIG. 4. QMC calculations for the hydrogen chain. (a) Extrapolations of atomic energies as a function of the supercell's length for metallic, EI CDW, and dimerized states. In the inset the energy differences are reported in eV with respect to the dimerized state. (b) Residual forces in the EI CDW state per atom. In the inset the residual forces for a 48 hydrogen atoms' supercell.

the extrapolation displayed in Fig. 4, which is analogous to Fig. 3 shown for the carbon atoms. In these extrapolations the exponential c parameter is ≈2. The energies per hydrogen atom of the metallic phase are lower than those obtained from previous VMC calculations in Ref. [57] confirming the accuracy of our basis set.

The EI CDW configuration is more stable than the ME one by about 0.013(2) eV while the relaxed DI chain gains an energy per atom of 0.347(2) eV. In the bottom panel of the same figure the essentially linear extrapolation of the residual forces per atom in the EI CDW phase, 0.0234(4) a.u., is reported. In the inset of the same panel we can see how the forces for the 48 hydrogen atom chain are equal in intensity and opposite in sign, as expected for the EI CDW phase.

These results confirm that also the ground state of the equidistant hydrogen chain is actually that of an insulator with a CDW (i.e., EI CDW). As in the case of the carbon chain, the forces will lead to a displacement of the atoms and thus to an additional energy gain via periodic lattice deformation. However, already on the purely electronic level (without displacing

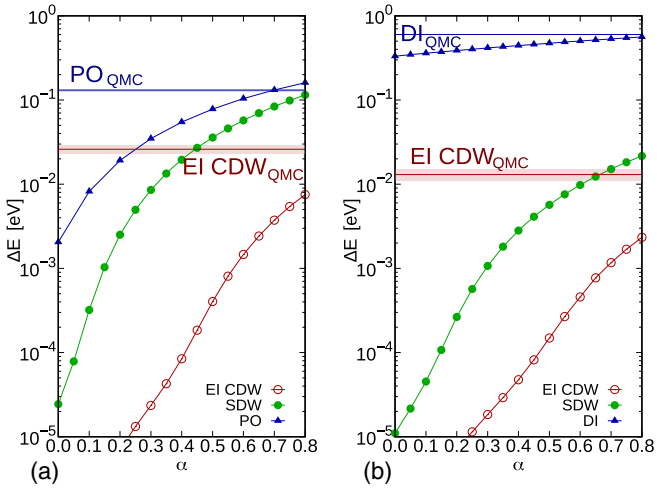

FIG. 5. Energy gain with respect to the metallic phase in the case of the carbon chain (a) and the hydrogen chain (b), for the CDW/PLD phase (blue triangles), referred to as PO in the case of carbon and DI in the case of hydrogen, the EI CDW phase (red circles), and the SDW phase (green circles). QMC references are represented through horizontal lines.

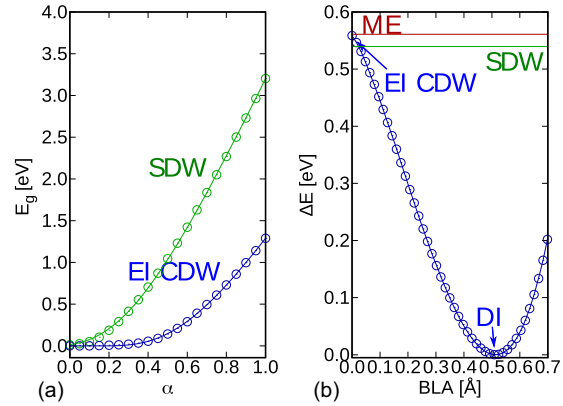

FIG. 6. Hydrogen chain. (a) Band gap E_g as a function of α for the EI CDW (blue circles) and SDW (green circles) phases. The continuous line is the fit of the *ab initio* data through Eq. (7) in the main text; the parameters of the interpolation are equal to $\xi_0 = 1.90\,\text{eV}$, $\gamma = 1.63$, and $\beta = 0.1$ for the EI CDW data and to $\xi_0 = 2.96\,\text{eV}$, $\gamma = 1.63$, and $\beta = -0.17$ for the SDW. (b) Ground state energy of the CDW/PLD phase as a function of the BLA evaluated at $\alpha = 0.8$. The red and green lines refer to the energy of the ME and SDW phases, respectively. In the plot the zero is fixed at the energy of the dimerized phase.

the atoms from their position in the monatomic linear chain) both carbon and hydrogen chains display a CDW regime.

We investigate the stability of the CDW/PLD, SDW, and EI CDW solutions with respect to the semimetallic phase as a function of $\alpha \in [0:1]$ keeping α_0 and ω fixed at the standard values of 0.16 and 0.33, respectively. The ground state energy of the different phases has been evaluated for each value of α always relaxing the lattice parameter and the BLA except for the EI CDW and SDW phases where the BLA was fixed at zero. We note that the EI CDW phase is not automatically obtained with the CRYSTAL17 code, because the self-consistent calculation starts with a symmetric charge distribution which remains symmetric in the course of the calculation even if the calculation is performed in a two-atom supercell. However, displacing one of the atoms by a very small amount for the first cycle and then placing it back into the symmetric position leads to a breaking of the symmetry of the electron density which is consequently preserved in the calculation since it leads to a lower energy state.

Our results are summarized in Fig. 5(b), where we show the behavior of the energy gain with respect to the semimetallic phase for the three configurations as a function of α. As seen for the carbon chain [Fig. 5(a)], also in this case the agreement with the QMC results can be found for large values of the α parameter (i.e., $\alpha = 0.8$), for which we obtain a lattice constant of 1.985 Å and a BLA of 0.512 Å.

This large value of α is consistent with the fact that in low-dimensional systems the screening of the long-range part of the Coulomb potential is strongly reduced. As a consequence the exchange interaction is strong enough to destabilize the semimetallic electronic structure with respect to the EI CDW and SDW phases [see Fig. 6(a)]. This latter, which can also be interpreted as an EI in the triplet channel, is more stable than the EI CDW. However, the charge ordering is stabilized with respect to the SDW when the ions are allowed to relax [see Fig. 6(b)].

APPENDIX B: GAP EQUATION FROM THE KOHN-SHAM HAMILTONIAN

In the following we will provide a direct link between our DFT calculation and the EI picture of the CDW phase transition. We start from a nonlocal KS Hamiltonian in the presence of an external perturbation $\Delta_{\text{ext}}(\mathbf{r})$ that breaks down the symmetry inducing a lower periodicity characterized by a wave vector $\mathbf{q}$: $\hat{H} = \int d\mathbf{r}\, d\mathbf{r}'\, \Psi^\dagger(\mathbf{r}) h(\mathbf{r}, \mathbf{r}') \Psi(\mathbf{r}')$, with the following definition of h:

$$h(\mathbf{r}, \mathbf{r}') = -\frac{\nabla^2}{2} + v(\mathbf{r}) + \Delta_{\text{ext}}(\mathbf{r}) + v_H(\mathbf{r}) + v_{xc}(\mathbf{r}, \mathbf{r}'), \tag{B1}$$

where v, v_H, and v_{xc} denote the ion, Hartree, and the nonlocal exchange-correlation potentials, respectively. The latter, in the case of hybrid functionals, can be formally written as the sum of a nonlocal exchange term v_x^{NL} which is a functional of the KS density matrix $\rho(\mathbf{r}, \mathbf{r}')$, a local exchange-correlation term v_{xc}^{L} (evaluated in GGA or LDA) and its exchange part, both related to the charge density $\rho(\mathbf{r}) = \rho(\mathbf{r}, \mathbf{r})$:

$$\begin{aligned} v_{xc}(\mathbf{r}, \mathbf{r}') = v_{xc}^{L}(\mathbf{r}) &+ \alpha_0 \left[v_{x;SR}^{NL}(\mathbf{r}, \mathbf{r}'; \omega) - v_{x;SR}^{L}(\mathbf{r}; \omega) \right] \\ &+ \alpha \left[v_{x;LR}^{NL}(\mathbf{r}, \mathbf{r}'; \omega) - v_{x;LR}^{L}(\mathbf{r}; \omega) \right], \end{aligned} \tag{B2}$$

where, according to Eq. (1), both v_x^{NL} and v_x^{L} have been separated in a short-range (SR) and a long-range (LR) contribution. Now we indicate with ρ_0 the density (or density matrix) of the unperturbed system and we introduce the induced density $\Delta\rho = \rho - \rho_0$. According to this definition, h can be separated into an unperturbed part h_0 (evaluated at $\Delta_{\text{ext}} = 0$) and a term Δh:

$$h_0(\mathbf{r}, \mathbf{r}') = -\frac{\nabla^2}{2} + v(\mathbf{r}) + v_H^0(\mathbf{r}) + v_{xc}^0(\mathbf{r}, \mathbf{r}'), \tag{B3}$$

$$\Delta h(\mathbf{r}, \mathbf{r}') = \Delta_{\text{ext}}(\mathbf{r}) + \Delta v_H(\mathbf{r}) + \Delta v_{xc}(\mathbf{r}, \mathbf{r}'), \tag{B4}$$

where v_H^0 and v_{xc}^0 are the Hartree and xc potentials evaluated at ρ_0 while $\Delta v_H(\mathbf{r})$ and $\Delta v_{xc}(\mathbf{r},\mathbf{r}')$ are given by the following expressions:

$$\Delta v_H(\mathbf{r}) = \int d\mathbf{r}' \frac{\Delta\rho(\mathbf{r}')}{|\mathbf{r}-\mathbf{r}'|}, \tag{B5}$$

$$\begin{aligned}\Delta v_{xc}(\mathbf{r},\mathbf{r}') = \int d\mathbf{r}'' \big[& f_{xc}^L(\mathbf{r},\mathbf{r}'') - \alpha_0 f_{x;SR}^L(\mathbf{r},\mathbf{r}'';\omega) \\ & - \alpha f_{x;LR}^L(\mathbf{r},\mathbf{r}'';\omega)\big]\Delta\rho(\mathbf{r}'')\delta(\mathbf{r}-\mathbf{r}') \\ & + \big[\alpha_0 f_{x;SR}^{NL}(\mathbf{r},\mathbf{r}';\omega) + \alpha f_{x;LR}^{NL}(\mathbf{r},\mathbf{r}';\omega)\big]\Delta\rho(\mathbf{r},\mathbf{r}');\end{aligned} \tag{B6}$$

here we take the linear approximation for Δv_{xc}. Expanding in the KS eigenfunctions of h_0 $[\phi_{i\mathbf{k}}(\mathbf{r})]$ we obtain

$$\begin{aligned}\hat{H} = & \sum_{ij\mathbf{k}} \big[\epsilon_{i\mathbf{k}}^0 \delta_{ij} + \Delta h_{i\mathbf{k},j\mathbf{k}}\big] c_{i\mathbf{k}}^\dagger c_{j\mathbf{k}} \\ & + \sum_{ij\mathbf{k}} \Delta h_{i\mathbf{k},j\mathbf{k}+\mathbf{q}} c_{i\mathbf{k}}^\dagger c_{j\mathbf{k}+\mathbf{q}}\end{aligned} \tag{B7}$$

with the obvious definition of the matrix elements:

$$\Delta h_{i\mathbf{k},j\mathbf{k}'} = \int d\mathbf{r}\, d\mathbf{r}' \phi_{i\mathbf{k}}^*(\mathbf{r}) \Delta h(\mathbf{r},\mathbf{r}') \phi_{j\mathbf{k}'}(\mathbf{r}').$$

In particular, in the simple case of a system consisting of a single half-filled band, Eq. (B7) becomes

$$\begin{aligned}\hat{H} = & \sum_{\mathbf{k}} \tilde{\epsilon}_{\mathbf{k}} c_{\mathbf{k}}^\dagger c_{\mathbf{k}} + \sum_{\mathbf{k}} \tilde{\epsilon}_{\mathbf{k}+\mathbf{q}} c_{\mathbf{k}+\mathbf{q}}^\dagger c_{\mathbf{k}+\mathbf{q}} \\ & - \left[\sum_{\mathbf{k}} \Delta_{\mathbf{k}} c_{\mathbf{k}}^\dagger c_{\mathbf{k}+\mathbf{q}} + \text{c.c.}\right].\end{aligned} \tag{B8}$$

Here the sum over $\mathbf{k}$ is restricted to the occupied states. Moreover we have introduced the quantities $\tilde{\epsilon}_{\mathbf{k}} = \epsilon_{\mathbf{k}}^0 + \Delta h_{\mathbf{k},\mathbf{k}}$ and the effective field $\Delta_{\mathbf{k}} = -\Delta h_{\mathbf{k},\mathbf{k}+\mathbf{q}}$. The Hamiltonian in Eq. (B8) has a simple bilinear form that can be trivially diagonalized using the following Bogoliubov–de Gennes-like transformation:

$$\begin{aligned}\alpha_{\mathbf{k}} &= v_{\mathbf{k}} c_{\mathbf{k}+\mathbf{q}} + u_{\mathbf{k}}^* c_{\mathbf{k}}, \\ \beta_{\mathbf{k}} &= u_{\mathbf{k}} c_{\mathbf{k}+\mathbf{q}} - v_{\mathbf{k}}^* c_{\mathbf{k}},\end{aligned} \tag{B9}$$

where $v_{\mathbf{k}}$ and $u_{\mathbf{k}}$ are the KS electron and hole amplitude and are given by the following relations: $u_{\mathbf{k}} = \sqrt{\frac{1}{2}(1+\frac{\xi_{\mathbf{k}}}{E_{\mathbf{k}}})}$ and $v_{\mathbf{k}} = \sqrt{\frac{1}{2}(1-\frac{\xi_{\mathbf{k}}}{E_{\mathbf{k}}})}$, with $\xi_{\mathbf{k}} = \frac{1}{2}(\tilde{\epsilon}_{c\mathbf{k}} - \tilde{\epsilon}_{v\mathbf{k}})$ and $E_{\mathbf{k}} = \sqrt{\xi_{\mathbf{k}}^2 + \Delta_{\mathbf{k}}^2}$. The eigenvalues of $\hat{H}$ become $\epsilon_{\mathbf{k}} = \frac{1}{2}(\tilde{\epsilon}_{c\mathbf{k}} + \tilde{\epsilon}_{v\mathbf{k}}) \pm E_{\mathbf{k}}$ and are characterized by a gap opening at $\mathbf{k} = \frac{\pi}{2a}$ with the value $2\Delta_{\mathbf{k}=\frac{\pi}{2a}}$ while $\Delta\rho$ takes the following expression:

$$\begin{aligned}\Delta\rho(\mathbf{r},\mathbf{r}') = & \sum_{\mathbf{k}} |v_{\mathbf{k}}|^2 [\phi_{\mathbf{k}+\mathbf{q}}^*(\mathbf{r}')\phi_{\mathbf{k}+\mathbf{q}}(\mathbf{r}) - \phi_{\mathbf{k}}^*(\mathbf{r}')\phi_{\mathbf{k}}(\mathbf{r})] \\ & + \sum_{\mathbf{k}} [u_{\mathbf{k}}^* v_{\mathbf{k}}^* \phi_{\mathbf{k}}^*(\mathbf{r}')\phi_{\mathbf{k}+\mathbf{q}}(\mathbf{r}) + u_{\mathbf{k}} v_{\mathbf{k}} \phi_{\mathbf{k}+\mathbf{q}}^*(\mathbf{r}')\phi_{\mathbf{k}}(\mathbf{r})].\end{aligned} \tag{B10}$$

Inserting Eq. (B10) in the expression of Δh we find that $\Delta h_{\mathbf{k},\mathbf{k}}$ is proportional to $|v_{\mathbf{k}}|^2$ and thus is negligible when $\Delta_{\mathbf{k}}$ is small enough so that $\tilde{\epsilon}_{\mathbf{k}} \approx \epsilon_{\mathbf{k}}^0$. Moreover from the expression of $\Delta h_{\mathbf{k},\mathbf{k}+\mathbf{q}}$ with $\Delta_{\text{ext}} \to 0$ we obtain the following equation for $\Delta_{\mathbf{k}}$:

$$\Delta_{\mathbf{k}} = -\frac{1}{2} \sum_{\mathbf{k}'} \mathcal{K}_{\mathbf{k},\mathbf{k}'} \frac{\Delta_{\mathbf{k}'}}{E_{\mathbf{k}'}} \tag{B11}$$

with

$$\mathcal{K}_{\mathbf{k},\mathbf{k}'} = 2v_{\mathbf{k},\mathbf{k}'} + f_{xc\mathbf{k},\mathbf{k}'}^L + \alpha_0\big[f_{x;SR\mathbf{k},\mathbf{k}'}^{NL}(\omega) - f_{x;SR\mathbf{k},\mathbf{k}'}^L(\omega)\big] + \alpha\big[f_{x;LR\mathbf{k},\mathbf{k}'}^{NL}(\omega) - f_{x;LR\mathbf{k},\mathbf{k}'}^L(\omega)\big] \tag{B12}$$

and with the following definition of the kernel matrix elements:

$$\begin{aligned}v_{\mathbf{k},\mathbf{k}'} &= \int d\mathbf{r}\, d\mathbf{r}' \phi_{\mathbf{k}}^*(\mathbf{r})\phi_{\mathbf{k}+\mathbf{q}}(\mathbf{r}) \frac{1}{|\mathbf{r}-\mathbf{r}'|} \phi_{\mathbf{k}'+\mathbf{q}}^*(\mathbf{r}')\phi_{\mathbf{k}'}(\mathbf{r}'), \\ f_{xc\mathbf{k},\mathbf{k}'}^L &= \int d\mathbf{r}\, d\mathbf{r}' \phi_{\mathbf{k}}^*(\mathbf{r})\phi_{\mathbf{k}+\mathbf{q}}(\mathbf{r}) f_{xc}^L(\mathbf{r},\mathbf{r}') \phi_{\mathbf{k}'+\mathbf{q}}^*(\mathbf{r}')\phi_{\mathbf{k}'}(\mathbf{r}'), \\ f_{x;SR\mathbf{k},\mathbf{k}'}^L(\omega) &= \int d\mathbf{r}\, d\mathbf{r}' \phi_{\mathbf{k}}^*(\mathbf{r})\phi_{\mathbf{k}+\mathbf{q}}(\mathbf{r}) f_{x;SR}^L(\mathbf{r},\mathbf{r}';\omega) \phi_{\mathbf{k}'+\mathbf{q}}^*(\mathbf{r}')\phi_{\mathbf{k}'}(\mathbf{r}'), \\ f_{x;LR\mathbf{k},\mathbf{k}'}^L(\omega) &= \int d\mathbf{r}\, d\mathbf{r}' \phi_{\mathbf{k}}^*(\mathbf{r})\phi_{\mathbf{k}+\mathbf{q}}(\mathbf{r}) f_{x;LR}^L(\mathbf{r},\mathbf{r}';\omega) \phi_{\mathbf{k}'+\mathbf{q}}^*(\mathbf{r}')\phi_{\mathbf{k}'}(\mathbf{r}'), \\ f_{x;SR\mathbf{k},\mathbf{k}'}^{NL}(\omega) &= \int d\mathbf{r}\, d\mathbf{r}' \phi_{\mathbf{k}}^*(\mathbf{r})\phi_{\mathbf{k}+\mathbf{q}}(\mathbf{r}') f_{x;SR}^{NL}(\mathbf{r},\mathbf{r}';\omega) \phi_{\mathbf{k}'+\mathbf{q}}^*(\mathbf{r}')\phi_{\mathbf{k}'}(\mathbf{r}), \\ f_{x;LR\mathbf{k},\mathbf{k}'}^{NL}(\omega) &= \int d\mathbf{r}\, d\mathbf{r}' \phi_{\mathbf{k}}^*(\mathbf{r})\phi_{\mathbf{k}+\mathbf{q}}(\mathbf{r}') f_{x;LR}^{NL}(\mathbf{r},\mathbf{r}';\omega) \phi_{\mathbf{k}'+\mathbf{q}}^*(\mathbf{r}')\phi_{\mathbf{k}'}(\mathbf{r}).\end{aligned}$$

Finally remembering that the expression for total energy in terms of the density (or density matrix) is

$$E[\rho] = 2\sum_i \epsilon_i - \frac{1}{2}\int d\mathbf{r} \int d\mathbf{r}' \frac{\rho(\mathbf{r})\rho(\mathbf{r}')}{|\mathbf{r}-\mathbf{r}'|} + E_{xc}[\rho] - \int d\mathbf{r}\, d\mathbf{r}' v_{xc}[\rho](\mathbf{r},\mathbf{r}')\rho(\mathbf{r},\mathbf{r}') \tag{B13}$$

we find that the energy variation at the first order in $\Delta\rho$ is given by $\Delta E = 2\sum_{\mathbf{k}}(\xi_{\mathbf{k}} - \sqrt{\xi_{\mathbf{k}}^2 + \Delta_{\mathbf{k}}^2})$.

Now we consider a simple model where the kernel of Eq. (B11) is just a constant $\bar{\mathcal{K}}$ (i.e., its average value on the Fermi surface) in an energy window ξ_0 around the Fermi level and zero elsewhere. Moreover, we assume that the band dispersion is linear around the Fermi surface so that $\xi_{\mathbf{k}} = v_F(|\mathbf{k}| - \frac{\pi}{2a})$, v_F being the Fermi velocity. Under these conditions the gap is just a constant Δ for $\xi < \xi_0$ and zero elsewhere and is given by

$$-\frac{4\pi v_F}{\bar{\mathcal{K}}} = \int_0^{\xi_0} d\xi \frac{1}{\sqrt{\xi^2 + \Delta^2}} \tag{B14}$$

so that

$$\Delta = -\frac{\xi_0}{\sinh\left(\frac{4\pi v_F}{\bar{\mathcal{K}}}\right)} \tag{B15}$$

or in terms of α:

$$\Delta = -\frac{\xi_0}{\sinh\left(\frac{\gamma}{\beta-\alpha}\right)}, \tag{B16}$$

where

$$\beta = \frac{2\bar{v} + \bar{f}^L_{xc} + \alpha_0\left[\bar{f}^{NL}_{x;SR}(\omega) - \bar{f}^L_{x;SR}(\omega)\right]}{\bar{f}^L_{x;LR}(\omega) - \bar{f}^{NL}_{x;LR}(\omega)} \tag{B17}$$

and

$$\gamma = \frac{4\pi v_F}{\bar{f}^L_{x;LR}(\omega) - \bar{f}^{NL}_{x;LR}(\omega)}. \tag{B18}$$

Moreover $\bar{v}$, $\bar{f}^L_{xc}$, $\bar{f}^L_x$, and $\bar{f}^{NL}_x$ are defined according to $\bar{\mathcal{K}}$. Since γ is a positive quantity, Eq. (B16) allows for nontrivial solutions only if $\alpha > \beta$.

[1] K. Rossnagel, J. Phys.: Condens. Matter **23**, 213001 (2011).
[2] R. Peierls, *More Surprises in Theoretical Physics* (Princeton University Press, Princeton, NJ, 1991).
[3] R. Peierls, Ann. Phys. **395**, 1055 (1929).
[4] A. W. Overhauser, Phys. Rev. Lett. **4**, 462 (1960); Phys. Rev. **167**, 691 (1968); Phys. Rev. B **29**, 7023 (1984).
[5] L. V. Keldysh and Y. V. Kopaev, Sov. Phys. Solid State. **6**, 2219 (1965).
[6] D. Jérome, T. M. Rice, and W. Kohn, Phys. Rev. **158**, 462 (1967).
[7] B. I. Halperin and T. M. Rice, Solid State Phys. **21**, 115 (1968).
[8] B. Bucher, P. Steiner, and P. Wachter, Phys. Rev. Lett. **67**, 2717 (1991).
[9] F. J. Di Salvo, D. E. Moncton, and J. V. Waszczak, Phys. Rev. B **14**, 4321 (1976).
[10] A. Kogar, M. S. Rak, S. Vig, A. A. Husain, F. Flicker, Y. I. Joe, L. Venema, G. J. MacDougall, T. C. Chiang, E. Fradkin, J. van Wezel, and P. Abbamonte, Science **358**, 1314 (2017).
[11] T. M. Rice, Solid State Phys. **32**, 1 (1977).
[12] J. E. Drut and T. A. Lähde, Phys. Rev. Lett. **102**, 026802 (2009).
[13] A. S. Rodin and A. H. Castro Neto, Phys. Rev. B **88**, 195437 (2013).
[14] D. Varsano, S. Sorella, D. Sangalli, M. Barborini, S. Corni, E. Molinari, and M. Rontani, Nat. Commun. **8**, 1461 (2017).
[15] M. Hellgren, J. Baima, and A. Acheche, Phys. Rev. B **98**, 201103(R) (2018).
[16] M. J. Rice and Y. N. Gartstein, J. Phys.: Condens. Matter **17**, 4615 (2005).
[17] M. J. Rice, Synth. Met. **141**, 9 (2004).
[18] M. J. Rice and Y. N. Gartstein, Synth. Met. **141**, 11 (2004).
[19] W. M. C. Foulkes, L. Mitas, R. J. Needs, and G. Rajagopal, Rev. Mod. Phys. **73**, 33 (2001).
[20] J. Kolorenč and L. Mitas, Rep. Prog. Phys. **74**, 026502 (2011).
[21] F. Becca and S. Sorella, *Quantum Monte Carlo Approaches for Correlated Systems* (Cambridge University Press, Cambridge, UK, 2017).
[22] K. Nakano, C. Attaccalite, M. Barborini, L. Capriotti, M. Casula, E. Coccia, M. Dagrada, C. Genovese, Y. Luo, G. Mazzola, A. Zen, and S. Sorella, J. Chem. Phys. **152**, 204121 (2020).
[23] M. Casula and S. Sorella, J. Chem. Phys. **119**, 6500 (2003).
[24] M. Casula, C. Attaccalite, and S. Sorella, J. Chem. Phys. **121**, 7110 (2004).
[25] F. Sterpone, L. Spanu, L. Ferraro, S. Sorella, and L. Guidoni, J. Chem. Theory Comput. **4**, 1428 (2008).
[26] J. Bardeen, L. N. Cooper, and J. R. Schrieffer, Phys. Rev. **106**, 162 (1957).
[27] A. J. Coleman, Rev. Mod. Phys. **35**, 668 (1963).
[28] A. J. Coleman, J. Math. Phys. **6**, 1425 (1965).
[29] C. Attaccalite and S. Sorella, Phys. Rev. Lett. **100**, 114501 (2008).
[30] M. Dagrada, S. Karakuzu, V. L. Vildosola, M. Casula, and S. Sorella, Phys. Rev. B **94**, 245108 (2016).
[31] A. Zen, E. Coccia, S. Gozem, M. Olivucci, and L. Guidoni, J. Chem. Theory Comput. **11**, 992 (2015).
[32] M. Barborini and L. Guidoni, J. Chem. Theory Comput. **11**, 508 (2015).
[33] M. Barborini and E. Coccia, J. Chem. Theory Comput. **11**, 5696 (2015).
[34] M. Marchi, S. Azadi, C. Casula, and S. Sorella, J. Chem. Phys. **131**, 154116 (2009).
[35] M. Burkatzki, C. Filippi, and M. Dolg, J. Chem. Phys. **126**, 234105 (2007).
[36] C. J. Umrigar, J. Toulouse, C. Filippi, S. Sorella, and R. G. Hennig, Phys. Rev. Lett. **98**, 110201 (2007).
[37] J. Toulouse and C. J. Umrigar, J. Chem. Phys. **126**, 084102 (2007).
[38] S. Sorella, M. Casula, and D. Rocca, J. Chem. Phys. **127**, 014105 (2007).
[39] S. Sorella and S. Capriotti, J. Chem. Phys. **133**, 234111 (2010).
[40] M. Barborini, S. Sorella, and L. Guidoni, J. Chem. Theory Comput. **8**, 1260 (2012).
[41] R. Dovesi, A. Erba, R. Orlando, C. M. Zicovich-Wilson, B. Civalleri, L. Maschio, M. Rérat, S. Casassa, J. Baima, S. Salustro, and B. Kirtman, WIREs Comput. Mol. Sci. **8**, e1360 (2018).
[42] M. F. Peintinger, D. V. Oliveira, and T. Bredow, J. Comput. Chem. **34**, 451 (2013).
[43] T. Yanai, D. P. Tew, and N. C. Handy, Chem. Phys. Lett. **393**, 51 (2004).

[44] S. Yang and M. Kertesz, J. Phys. Chem. A **110**, 9771 (2006).
[45] S. Yang, M. Kertesz, V. Zólyomi, and J. Kürti, J. Phys. Chem. A **111**, 2434 (2007).
[46] P. A. Apgar and K. C. Yee, Acta Crystallogr., Sect. B: Struct. Sci. **34**, 957 (1978).
[47] A. Kobayashi, H. Kobayashi, Y. Tokura, T. Kanetake, and T. Koda, J. Chem. Phys. **87**, 4962 (1987).
[48] D. Kobelt and E. F. Paulus, Acta Crystallogr., Sect. B: Struct. Sci. **30**, 232 (1974).
[49] E. Mostaani, B. Monserrat, N. D. Drummond, and C. J. Lambert, Phys. Chem. Chem. Phys. **18**, 14810 (2016).
[50] M. Barborini and L. Guidoni, J. Chem. Theory Comput. **11**, 4109 (2015).
[51] S. Refaely-Abramson, M. Jain, S. Sharifzadeh, J. B. Neaton, and L. Kronik, Phys. Rev. B **92**, 081204(R) (2015).
[52] M. E. Casida, Time-dependent density functional response theory for molecules, in *Recent Advances in Density Functional Methods* (World Scientific, Singapore, 1995), pp. 155–192.
[53] M. D. Johannes and I. I. Mazin, Phys. Rev. B **77**, 165135 (2008).
[54] P. Ghosez, X. Gonze, and R. W. Godby, Phys. Rev. B **56**, 12811 (1997).
[55] D. Varsano, A. Marini, and A. Rubio, Phys. Rev. Lett. **101**, 133002 (2008).
[56] M. Kertesz, J. Koller, and A. Ažman, J. Chem. Phys. **68**, 2779 (1978); **69**, 2937 (1978); M. Kertész, J. C. V. Koller, and A. Ažman, Phys. Rev. B **19**, 2034 (1979).
[57] L. Stella, C. Attaccalite, S. Sorella, and A. Rubio, Phys. Rev. B **84**, 245117 (2011).